Inorg. Chem. **2004**, *43*, 7421–7430

Molecular Design of Luminescence Ion Probes for Various Cations Based on Weak Gold(I)···Gold(I) Interactions in Dinuclear Gold(I) Complexes

Chi-Kwan Li, Xiao-Xia Lu, Keith Man-Chung Wong, Chui-Ling Chan, Nianyong Zhu, and Vivian Wing-Wah Yam*

Open Laboratory of Chemical Biology of the Institute of Molecular Technology for Drug Discovery and Synthesis, Centre for Carbon-Rich Molecular and Nanoscale Metal-Based Materials Research, and Department of Chemistry, The University of Hong Kong, Pokfulam Road, Hong Kong SAR, People's Republic of China

Received July 9, 2004

A series of luminescent dinuclear gold(I) complexes with different crown ether pendants, $[Au_2(P\wedge P)(S\text{-}B15C5)_2]$ [S-B15C5 = 4′-mercaptobenzo-15-crown-5, P^P = bis(dicyclohexylphosphino)methane (dcpm) (**1**), bis(diphenylphosphino)methane (dppm) (**2**)] and $[Au_2(P\wedge P)(S\text{-}B18C6)_2]$ [S-B18C6 = 4′-mercaptobenzo-18-crown-6, P^P = dcpm (**3**), dppm (**4**)], and their related crown-free complexes, $[Au_2(P\wedge P)(SC_6H_3(OMe)_2\text{-}3,4)_2]$ [P^P = dcpm (**5**), dppm (**6**)], were synthesized. The low-energy emission of the mercaptocrown ether-containing gold(I) complexes are tentatively assigned as originated from states derived from a S → Au ligand-to-metal charge transfer (LMCT) transition. The crown ether-containing gold(I) complexes showed specific binding abilities toward various metal cations according to the ring size of the crown pendants. Spectroscopic evidence was provided for the metal-ion-induced switching on of the gold···gold interactions upon the binding of particular metal ions in a sandwich binding mode.

Introduction

Since the first discovery of macrocyclic crown polyethers by Pedersen et al.,[1] the study of their binding abilities toward alkali metal, alkaline earth metal, and transition metal ions has aroused much attention.[2] There are extensive applications of crown ethers in the field of metal ion probes, pH sensors, molecular recognitions, photocontrol of ion extractions and transport, and construction of chemical switches.[3] Although various types of luminescent chemosensors have been developed, most of them are mainly confined to systems that are organic in nature, while relatively little have been explored in the field of inorganic/organometallic compounds. Recently, there have been an increasing number of transition metal-based metalloreceptors reported which can provide spectroscopic detection upon ion-binding.[4−6] However, most of them were focused on systems with metal-to-ligand charge transfer (MLCT) excited states,[4,5] with relatively few studies or exploitations on other systems.[6]

Recently, there has been a growing interest in the study of polynuclear gold(I) complexes, in particular with regard to the phenomenon of aurophilicity associated with these complexes, which results from weak gold···gold interactions.[7,8] Gold(I) thiolates containing phosphine ligands

* Author to whom correspondence should be addressed. E-mail: wwyam@hku.hk. Tel.: (852)2859-2153. Fax: (852)2857-1586.

(1) Pedersen, C. J. *J. Am. Chem. Soc.* **1967**, *89*, 2495.
(2) Izatt, R. M.; Bradshaw, J. S.; Nielsen, S. A.; Lamb, J. D.; Christensen, J. J.; Sen, D. *Chem. Rev.* **1985**, *85*, 271.
(3) (a) Xia, W. S.; Schmehl, R. H.; Li, C. J. *Tetrahedron* **2000**, *56*, 7045. (b) Gunnlaugsson, T.; Davis, A. P.; Glynn, M. *Chem. Commun.* **2001**, 2556. (c) Valeur, B.; Leray, I. *Coord. Chem. Rev.* **2000**, *205*, 3. (d) Lehn, J. M. *Angew. Chem., Int. Ed. Engl.* **1988**, *27*, 89. (e) Gokel, G. W.; Mukhopadhyay, A. *Chem. Soc. Rev.* **2001**, *30*, 274.
(4) (a) MacQueen D. B.; Schanze, K. S. *J. Am. Chem. Soc*. **1991**, *113*, 6108. (b). Shen, Y.; Sullivan, B. P. *Inorg. Chem*. **1995**, *34*, 6235. (c) Bushell, K. L.; Couchman, S. M.; Jeffery, J. C.; Ress, L. H.; Ward, M. D. *J. Chem. Soc., Dalton Trans.* **1998**, 3397. (d) Encinas, S.; Bushell, K. L.; Couchman, S. M.; Jeffery, J. C.; Ward, M. D.; Flamigni, L.; Barigelletti, F. *J. Chem. Soc., Dalton Trans.* **2000**, 1783.
(5) (a) Yam, V. W. W.; Lee, V. W. M. *J. Chem. Soc., Dalton Trans.* **1997**, 3005. (b) Yam, V. W. W.; Lee, V. W. M.; Ke, F.; Siu, K. W. M. *Inorg. Chem.* **1997**, *36*, 2124. (c) Yam, V. W. W.; Tang, R. P. L.; Wong, K. M. C.; Cheung, K. K. *Organometallics* **2001**, *20*, 4476. (d) Yam, V. W. W.; Pui, Y. L.; Cheung, K. K. *Inorg. Chim. Acta* **2002**, *335*, 77.
(6) (a) Yam, V. W. W.; Tang, R. P. L.; Wong, K. M. C.; Ko, C. C.; Cheung, K. K. *Inorg. Chem.* **2001**, *40*, 571. (b) Yam, V. W. W.; Pui, Y. L.; Cheung, K. K.; Zhu, N. *New. J. Chem.* **2002**, *26*, 536. (c) Yam, V. W. W.; Tang, R. P. L.; Wong, K. M. C.; Lu, X. X.; Cheung, K. K.; Zhu, N. *Chem.—Eur. J.* **2002**, *8*, 4066.

10.1021/ic049094u CCC: $27.50
Published on Web 10/14/2004

Chart 1

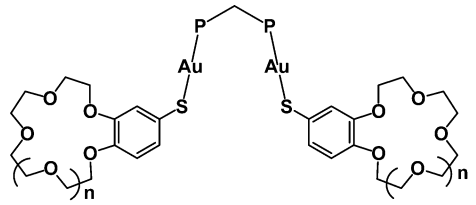

where P^P = dcpm, L = S-B15C5 (n =1) (**1**)
P^P = dppm, L = S-B15C5 (n =1) (**2**)
P^P = dcpm, L = S-B18C6 (n =2) (**3**)
P^P = dppm, L = S-B18C6 (n =2) (**4**)
P^P = dcpm, L = $SC_6H_3(OMe)_2$-3,4 (**5**)
P^P = dppm, L = $SC_6H_3(OMe)_2$-3,4 (**6**)

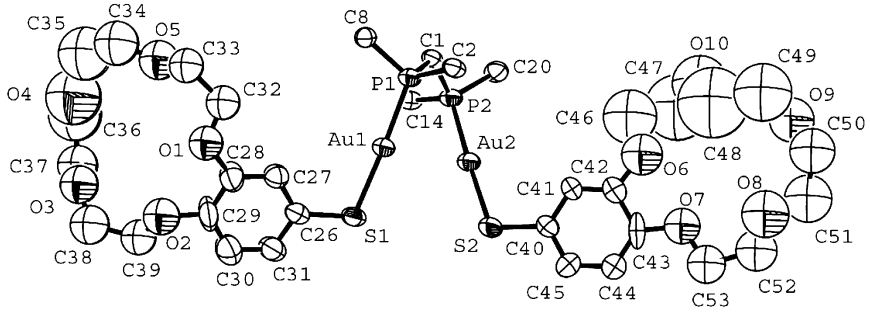

Figure 1. Perspective drawing of $[Au_2(dcpm)(S\text{-}B15C5)_2]$ (**1**) with atomic numbering scheme. Hydrogen atoms are omitted, and only the ipso carbons of the cyclohexyl rings are shown for clarity. Thermal ellipsoids are shown at the 30% probability level.

represent a class of polynuclear d^{10} metal complexes which exhibits rich luminescence properties.[9] In view of the rich spectroscopic and luminescence properties exhibited by gold(I) phosphine complexes, together with the unique and attractive property of Au···Au interactions resulting from aurophilicity, it is anticipated that the incorporation of macrocycles to dinuclear gold(I) building block would serve as an ideal candidate for the design of luminescence chemosensors as well as molecular optoelectronic switching devices based on the switching on and off of the gold···gold interactions. A series of dinuclear gold(I) crown ether-containing complexes which can act as luminescence ion probe for potassium ions have been reported by us previously.[10] These complexes demonstrated a novel concept of the utilization of the on/off switching of gold···gold interactions for metal ion sensing. To extend the work of the novel gold(I) complexes containing benzo-15-crown-5 moieties,[10] gold(I) phosphine thiolate complexes containing benzo-18-crown-6 pendants are synthesized, so as to investigate the effect of crown size on the specificity of metal ion-binding by such systems. Herein we report the synthesis of a series of dinuclear gold(I) complexes with different crown ether pendants, $[Au_2(P\text{^}P)(S\text{-}B15C5)_2]$ [S-B15C5 = 4′-mercaptobenzo-15-crown-5, P^P = bis(dicyclohexylphosphino)methane (dcpm) (**1**), bis(diphenylphosphino)methane (dppm) (**2**)] and $[Au_2(P\text{^}P)(S\text{-}B18C6)_2]$ [S-B18C6 = 4′-mercaptobenzo-18-crown-6, P^P = dcpm (**3**), dppm (**4**)], and their related crown-free analogues, $[Au_2(P\text{^}P)(SC_6H_3(OMe)_2\text{-}3,4)_2]$ [P^P = dcpm (**5**), dppm (**6**)]; the crystal structures of **1** and **3** have been determined. Complexes **1**, **2**, **5**, and **6** have previously been communicated. On the basis of a judicious choice of an appropriate size match between the crown ether moiety and the metal cations of interest, metal ion-binding in an intramolecular sandwich binding fashion has been demonstrated, as confirmed by ESI-mass spectrometry, when the size of the metal cations is larger than that of the crown ether cavities. Complexes **1**−**4** displayed low-energy ligand-to-metal−metal charge transfer (LMMCT) emission, which was induced upon the binding of metal cations that are larger than the size of the crown cavity. Their binding constants, log K_s, with various metal cations, i.e., K^+, Cs^+, and Rb^+, have been determined by UV−vis absorption and luminescence spectroscopies.

Results and Discussion

Syntheses and Characterization. Complexes **1**−**6** (Chart 1) were prepared by the direct ligand substitution reactions of $[Au_2(P\text{^}P)Cl_2]$ with the mercaptocrown ligand in the presence of triethylamine as the base. All the complexes are stable both in the solid state and in solution. Repeated recrystallization of the complexes from dichloromethane−diethyl ether to remove the triethylammonium chloride gave X-ray-quality single crystals of **1** and **3**, which have been structurally determined.

Crystal Structure Determination. Figures 1 and 2 show the perspective drawings of **1** and **3**, respectively. The respective crystal structure determination data and selected

(7) (a) Schmidbaur, H. *Gold Bull.* **1990**, *23*, 11. (b) Scherbaum, F.; Grohmann, A.; Huber, B.; Krüger, C.; Schmidbaur, H. *Angew. Chem., Int. Ed. Engl.* **1988**, *27*, 1544. (c) Pyykkö, P. *Chem. Rev.* **1997**, *97*, 597. (d) Jiang, Y.; Alvarez, S.; Hoffmann, R. *Inorg. Chem.* **1985**, *24*, 749. (e) Mingos, D. M. P. *J. Chem. Soc., Dalton Trans.* **1976**, 1163. (f) Harwell, D. E.; Mortimer, M. D.; Knobler, C. B.; Anet, F. A. L.; Hawthorne, M. F. *J. Am. Chem. Soc.* **1996**, *118*, 2679. (g) Narayanaswany, R.; Young, M. A.; Parkhurst, E.; Ouellette, M.; Kerr, M. E.; Ho, D. M.; Elder, R. C.; Bruce, A. E.; Bruce, M. R. M. *Inorg. Chem.* **1993**, *32*, 2506.
(8) Zhang, H. X.; Che, C. M. *Chem.—Eur. J.* **2001**, *7*, 4887.
(9) (a) Assefa, Z.; McBurnett, B. G.; Staples, R. J.; Fackler, J. P., Jr.; Assmann, B.; Angermaier, K.; Schmidbaur, H. *Inorg. Chem.* **1995**, *34*, 75. (b) Jones, W. B.; Yuan, J.; Narayanaswamy, R.; Young, M. A.; Elder, R. C.; Bruce, A. E.; Bruce, M. R. M. *Inorg. Chem.* **1995**, *34*, 1996. (c) Forward, J. M.; Bohmann, D.; Fackler, J. P., Jr.; Staples, R. J. *Inorg. Chem.* **1995**, *34*, 6330. (d) Hanna, S. D.; Zink, J. I. *Inorg. Chem.* **1996**, *35*, 297.
(10) (a) Yam, V. W. W.; Li, C. K.; Chan, C. L. *Angew. Chem., Int. Engl.* **1998**, *37*, 2857. (b) Yam, V. W. W.; Chan, C. L.; Li, C. K.; Wong, K. M. C. *Coord. Chem. Rev.* **2001**, *216*, 173.

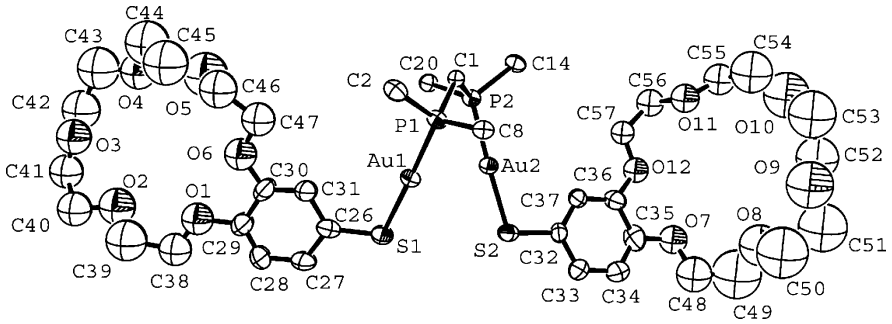

Figure 2. Perspective drawing of $[Au_2(dcpm)(S\text{-}B18C6)_2]$ (**3**) with atomic numbering scheme. Hydrogen atoms are omitted, and only the *ipso* carbons of the cyclohexyl rings are shown for clarity. Thermal ellipsoids are shown at the 30% probability level.

Table 1. Crystal and Structure Determination Data for **1** and **3**

	1	**3**
empirical formula	$C_{53}H_{84}Au_2O_{10}P_2S_2$	$C_{57}H_{92}Au_2O_{12}P_2S_2$
fw	1401.24	1487.28
temp (K)	301	293 (2)
wavelength (Å)	0.710 73	0.710 69
cryst system	monoclinic	monoclinic
space group	$P2_1/a$	$P2_1/c$
a (Å)	16.459(1)	18.934(4)
b (Å)	19.956(2)	20.287(4)
c (Å)	17.772(2)	16.638(3)
α (deg)	90	90
β (deg)	91.516(9)	91.51(3)
γ (deg)	90	90
V (Å^3)	5835.1(10)	6389(2)
Z	4	4
D(calcd) (mg m^{-3})	1.595	1.546
abs coeff (mm^{-1})	5.219	4.758
F(000)	2808	2992
cryst size (mm)	0.2 × 0.1 × 0.3	0.3 × 0.2 × 0.1
collecn range, $2\theta_{max}$ (deg)	50	50.68
index ranges	$0 \le h \le 19$	$-21 \le h \le 21$
	$0 \le k \le 23$	$-23 \le k \le 23$
	$-20 \le l \le 20$	$-18 \le l \le 17$
reflcns collcd	10 977	27 329
indpndt reflcns	10 587 [R(int) = 0.045]	9324 [R(int) = 0.0601]
no. of data for struct anal.	4415	4821
no. of params	307	545
goodness-of-fit on F^2	2.60	0.877
final R indices	$R_1 = 0.047$ [$I > 3\sigma(I)$]	$R_1 = 0.0475$ [$I > 2\sigma(I)$]
	$wR_2 = 0.0693$	$wR_2 = 0.1223$
largest diff peak and hole (e Å^{-3})	0.87, −0.84	1.270, −1.458

Table 2. Selected Bond Lengths (Å) and Angles (deg) with Estimated Standard Deviations (esd's) in Parentheses for **1** and **3**

	1	**3**
Au(1)−P(1)	2.262(4)	2.274(3)
Au(1)−S(1)	2.295(4)	2.301(3)
Au(1)···Au(2)	3.284(1)	3.2556(8)
Au(2)−P(2)	2.265(4)	2.267(3)
Au(2)−S(2)	2.292(5)	2.293(3)
S(1)−C(26)	1.72(2)	1.732(15)
S(2)−C(40)	1.75(2)	
S(2)−C(32)		1.788(12)
P(1)−Au(1)−S(1)	176.7(2)	178.25(13)
P(2)−Au(2)−S(2)	177.3(2)	177.77(12)
C(26)−S(1)−Au(1)	108.8(7)	109.1(4)
C(40)−S(2)−Au(2)	108.1(7)	
C(32)−S(2)−Au(2)		108.1(4)
C(1)−P(1)−Au(1)	115.2(5)	113.6(3)
C(1)−P(2)−Au(2)	113.0(5)	117.1(3)
C(8)−P(1)−Au(1)	111.3(5)	114.6(3)
C(2)−P(1)−Au(1)	113.4(5)	112.2(4)
C(20)−P(2)−Au(2)	111.9(6)	113.5(3)
C(14)−P(2)−Au(2)	115.1(5)	112.0(4)
P(2)−C(1)−P(1)	120.3(8)	116.3(5)

bond distances and angles are summarized in Tables 1 and 2. The molecular structures of complexes **1** and **3** are basically similar. Each gold atom of the complexes is two-coordinate, with one side bound to the sulfur atom of the thiolate group and the other side bound to the phosphorus atom of the diphosphine ligand. The two gold(I)−mercapto-crown ether moieties, bridged by a diphosphine ligand, are directed away from each other, probably to relieve the repulsion between the two sterically bulky crown ether pendants. The bond angles of P−Au−S in complex **1** are 178.25(13) and 177.77(12)°, while those of complex **3** are 178.25(13) and 177.77(12)°; all of them only show a slight deviation from ideal linearity, typical of the sp hybridization in gold(I). The intramolecular Au···Au separation of complex **3** (3.2256(8) Å) is slightly shorter than the benzo-15-crown-5 analogue **1** (3.28 Å), which indicates the presence of weak Au···Au interactions in both complexes in the solid state. It is likely that the steric requirement of the bulky crown ether pendants prevents shorter Au···Au contacts. The Au−S bond distances in the range of 2.301(3)−2.292(5) Å and Au−P distances of 2.274(3)−2.262(4) Å are normal and typical of two-coordinate gold(I) complexes.[9b] The angles of C(26)−S(1)−Au(1) and C(32)−S(2)−Au(2) are 109.1(4) and

Table 3. Electronic Absorption and Emission Spectral Data for the Mercaptocrown Ether-Containing Gold(I) Complexes

	emission	
abs [λ/nm (ϵ/dm^3 mol^{-1} cm^{-1})][a]	medium (T/K)	corrected [λ_{em}/nm (τ_o/μs)]
	complex **1**	
274 sh (20 200)	solid (298)	*b*
298 (15 700)	solid (77)	512
324 sh (9700)	CH_2Cl_2 (298)	520 (<0.1)
	CH_2Cl_2 (77)	620
	complex **2**	
266 (33 000)	solid (298)	650 (<0.1)
298 sh (16 000)	solid (77)	628
327 (5330)	CH_2Cl_2 (298)	580 (<0.1)
	CH_2Cl_2 (77)	645
	complex **3**	
273 sh (25 300)	solid (298)	*b*
298 (19 075)	solid (77)	508
341 sh (7100)	CH_2Cl_2 (298)	492 (<0.1)
	CH_2Cl_2 (77)	530
	complex **4**	
266 (32 680)	solid (298)	660 (<0.1)
302 sh (15 900)	solid (77)	601
336 (8105)	CH_2Cl_2 (298)	580 (<0.1)
	CH_2Cl_2 (77)	554
	complex **5**	
275 sh (23 500)	solid (298)	627 (<0.1)
300 (15 670)	solid (77)	647
330 sh (9300)	CH_2Cl_2 (298)	553 (<0.1)
	CH_2Cl_2 (77)	565
	complex **6**	
266 (32 570)	solid (298)	650 (<0.1)
302 sh (14 700)	solid (77)	640
332 (7740)	CH_2Cl_2 (298)	580 (<0.1)
	CH_2Cl_2 (77)	583

[a] Measured in dichloromethane at 298 K. [b] Nonemissive.

108.1(4)°, respectively, in complex **3**, while the angles of C(26)−S(1)−Au(1) and C(40)−S(2)−Au(2) are 108.8(7) and 108.1(7)°, respectively, in complex **1**. This indicates that the two crown moieties of each complex are directed away from each other. Moreover, due to the steric bulkiness of the cyclohexyl rings and the crown ether pendants, the shortest intermolecular Au···Au contact is longer than 8 Å in both complexes, which is too long for any interaction to be considered.

Electronic Absorption Spectroscopy. The electronic absorption spectra of all the complexes show high-energy absorption bands at ca. 266−302 nm and low-energy absorption shoulders at ca. 324−341 nm with tails extending to ca. 400 nm. The electronic absorption data for complexes **1**−**6** are summarized in Table 3. Basically, the electronic absorption spectra of complexes **3** and **4** are similar to that of their corresponding analogues **1** and **2**. In view of the similar absorption energies found in the corresponding chloro analogues, $Au_2(dcpm)Cl_2$ and $Au_2(dppm)Cl_2$, and in the free mercaptocrown ether ligands, the high-energy absorption bands are tentatively assigned as intraligand transitions of the diphosphine and mercaptocrown ether. The low-energy absorption shoulders, which are absent in the chloro analogues, $Au_2(dcpm)Cl_2$ and $Au_2(dppm)Cl_2$, are characteristic of the (thiolato)gold(I) phosphine system.[7g,11,12] Accordingly, the low-energy absorption shoulders are assigned to a thiolate-to-gold ligand-to-metal charge transfer (LMCT) transition and similar assignment has been reported in the related (thiolato)gold(I) phosphine system.[11] For the complexes with the same diphosphine ligands, i.e. **1**, **3**, and **5** with dcpm ligands and **2**, **4**, and **6** with dppm ligand, the close resemblance of their UV−visible absorption spectra is understandable since a variation in the size of the crown cavity or a modification to the methoxy groups in the crown-free analogues would have very little influence on the electronic effect and hence very little influence on the spectroscopic properties of the compounds.

Emission Properties. All the (thiolato)gold(I) phosphine complexes exhibit luminescence upon photoexcitation in dichloromethane solution or in the solid state. The measured lifetimes in the sub-microsecond range suggest that the emission is derived from a spin-forbidden transition and is probably of triplet parentage, giving rise to phosphorescence. The photophysical data are collected in Table 3. The emission bands at 492−580 nm observed in complexes **1**−**6** in dichloromethane solution at 298 K are assigned as derived from a S → Au LMCT origin, probably with minimal perturbation by Au···Au interactions. It is likely that any modification of this type would be insignificant given the relatively large Au···Au separations of 3.28 and 3.23 Å observed in the solid-state structures of **1** and **3**, respectively, the separations of which are believed to be even larger in solution due to the floppy nature of the molecule. When compared to similar systems containing significant interactions, the Au···Au separations are usually in the range of ca. 2.90− 3.00 Å.[7c,9b,13−16] The result matches well with the previous works of Fackler, Bruce, and Yam, in which the emission maxima for S → Au LMCT emissions of gold(I) thiolate complexes without Au···Au interactions are reported to be at ca. 480−520 nm.[7c,9b,13−16] Some modifications due to Au···Au interactions may exist in the solid state, leading to a slight red shift in the emission maxima. The excitation and emission spectra of **3** in dichloromethane at room temperature are depicted in Figure 3. The slightly lower emission energies of the complexes with the dppm than the dcpm-containing analogues are in accord with the poorer electron-donating ability of dppm than dcpm, rendering the Au(I) metal-centered acceptor orbital lower lying in energy,

(11) (a) El-Etri, M. M.; Scovell, W. M. *Inorg. Chem.* **1990**, *29*, 480. (b) Jaw, H. R. C.; Mason, W. R. *Inorg. Chem.* **1989**, *28*, 4370. (c) Savas, M. M.; Mason, W. R. *Inorg. Chem.* **1987**, *26*, 301. (d) Tzeng, B. C.; Chan, C. K.; Cheung, K. K.; Che, C. M.; Peng, S. M. *Chem. Commun.* **1997**, 135.

(12) Yam, V. W. W.; Cheng, E. C. C.; Zhou, Z. Y. *Angew. Chem., Int. Ed.* **2000**, *39*, 1683.

(13) (a) Vogler, A.; Kunkely, H. *Chem. Phys. Lett*. **1988**, *150*, 135. (b) Che, C. M.; Kwong, H. L.; Yam, V. W. W.; Cho, K. C. *Chem. Commun*. **1989**, 885. (c) Che, C. M.; Kwong, H. L.; Poon, C. K.; Yam, V. W. W. *J. Chem. Soc., Dalton Trans*. **1990**, 3215. (d) Yam, V. W. W.; Lee, W. K. *J. Chem. Soc., Dalton Trans.* **1993**, 2097.

(14) (a) Pyykkö, P.; Zhao, Y. *Angew. Chem., Int. Ed. Engl*. **1991**, *30*, 604. (b) Pyykkö, P.; Li, J.; Runeberg, N. *Chem. Phys. Lett.* **1994**, *218*, 133. (c) Görling, A.; Rösch, N.;. Ellis, D. E.; Schmidbaur, H. *Inorg. Chem.* **1991**, *30*, 3986. (d). Häberlen, O. D.; Schmidbaur, H.; Rösch, N. *J. Am. Chem. Soc.* **1994**, *116*, 8241. (e) Burdett, J. K.; Eisenstein, O.; Schweizer, W. B. *Inorg. Chem.* **1994**, *33*, 3261.

(15) (a) Jaw, H. C.; Savas, M.; Rogers, R. D.; Mason, W. R. *Inorg. Chem.* **1989**, *28*, 1028. (b) Chastain, S. K.; Mason, W. R. *Inorg. Chem.* **1982**, *21*, 1, 3717.

(16) Yam, V. W. W.; Lai, T. F.; Che, C. M. *J. Chem. Soc., Dalton Trans.* **1990**, 3747.

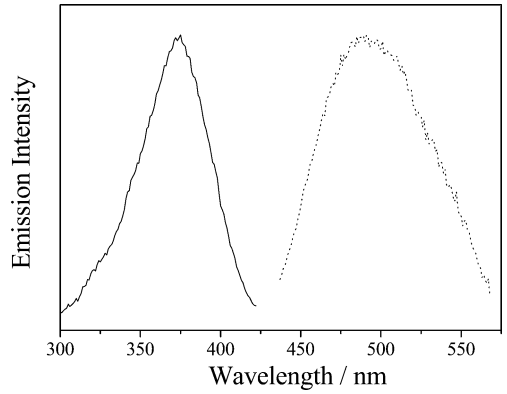

Figure 3. Excitation (—) and corrected emission (---) spectra of [Au_2(dcpm)(S-B18C6)$_2$] (**3**) in dichloromethane at room temperature.

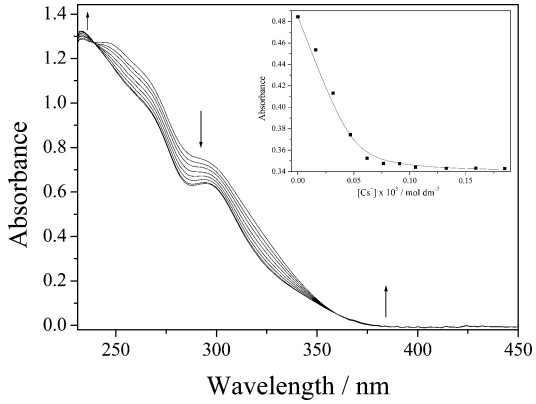

Figure 4. Electronic absorption spectral traces of [Au_2(dcpm)(S-B18C6)$_2$] (**3**) in CH_2Cl_2−MeOH (1:1 v/v) upon addition of CsOTf at 298 K. The inset shows a plot of absorbance vs [Cs^+] monitored at λ = 318 nm (■) and its theoretical fit (—).

leading to a lower energy emission of substantial LMCT character. Some mixing of a metal−pertubed intraligand phosphine phosphorescence may also be possible.

Cation Binding Studies. Unlike previous binding studies of complexes **1** and **2**,[6] in which their electronic absorption spectra in CH_2Cl_2−MeOH (1:1, v/v) mixture containing 0.1 mol dm^{-3} tetra-*n*-butylammonium hexafluorophosphate as supporting electrolyte show spectral changes upon addition of potassium hexafluorophosphate, no such spectral changes were observed for complexes **3** and **4** upon addition of potassium ion under the same condition. However, upon addition of cesium trifluoromethanesulfonate to **3** and **4**, spectral changes in the UV−vis absorption spectra were observed. The electronic absorption spectral traces of **3** upon addition of cesium ions are illustrated in Figure 4. The inset in Figure 4 shows the changes of absorbance at 318 nm as a function of Cs^+ ion concentration, reaching saturation at higher concentrations. Clean isosbestic points at 240 and 360 nm for **3** and at 256 and 320 nm for **4** were observed in the electronic absorption spectra, indicating that the reaction is clean and probably involves only two absorbing species in equilibrium present in the solution. Spectrochemical recognition of guest metal ions is confirmed by the absence of spectral changes in the absorption bands of the corresponding crown-free analogues, **5** and **6**, upon addition of metal ions under the same condition. The changes are ascribed to the specific association of metal cations to the polyether cavity of the complexes rather than resulting from changes in the solvent polarity.

Table 4. Binding Constants of Mercaptocrown Ether-Containing Gold(I) Complexes with Metal Cations Determined by UV−Vis Spectrophotometric Titration at 298 K

	binding consts, log K_s[a]		
complex	K^+	Rb^+	Cs^+
[Au_2(dcpm)(S-B15C5)$_2$] (**1**)	4.0[b]	3.4	3.4
[Au_2(dppm)(S-B15C5)$_2$] (**2**)	3.4[b] (3.2)	2.9 (2.9)	2.3 (2.6)
[Au_2(dcpm)(S-B18C6)$_2$] (**3**)	*c*	4.5	5.5
[Au_2(dppm)(S-B18C6)$_2$] (**4**)	*c*	*d*	4.6 (4.6)

[a] Binding constants, log K_s, are determined from UV−vis spectrophotometric method while data in parentheses are determined from emission spectrophotometric method. [b] From ref 6a. [c] Cannot be determined. [d] Not measured.

To gain more insight into the cation-binding properties of the complexes, stability constants (K_s) for the binding of metal ions to the complexes have been determined. Binding constants for 1:1 complexation were obtained by a nonlinear least-squares fit[17] of the absorbance versus the concentration of the metal ion added. The close agreement of the experimental data with the theoretical fits indicates that the complexation of a Cs^+ ion to the dinuclear Au(I) complex was in a 1:1 ratio. Since the ionic diameter of Cs^+ ion (3.34 Å) is too large to fit into the cavity size of a benzo-18-crown-6 (diameter: 2.6−3.2 Å), a 1:1 complexation ratio would indicate that the Cs^+ ion is sandwiched between two benzo-18-crown-6 units within the dinuclear Au(I) complex. Similar binding studies have been made for complexes **1**−**4** with CsOTf and RbOTf. The stability constants (K_s) for complexes **1**−**4** with various metal ions are summarized in Table 4. For complexes **1** and **2** with benzo-15-crown-5 pendants, the highest stability constant has been obtained in the case of binding of K^+. The absence of spectral change in complexes **3** and **4** with benzo-18-crown-6 pendants upon addition of Na^+ or K^+ is ascribed to the fact that no sandwich binding could occur because Na^+ or K^+ would be bound inside the benzo-18-crown-6 cavity.

The changes in the luminescence response of the dinuclear gold(I) complexes toward metal ion binding were found to be more strikingly pronounced. Figure 5a shows the corrected emission spectral changes of **4** with excitation at 320 nm which is the isosbestic wavelength upon addition of CsOTf. The band at ca. 410 nm showed a drop in intensity with the concomitant formation of a new low-energy emission band at ca. 790 nm upon addition of Cs^+ ions. An isoemissive point was obtained at ca. 590 nm. Similar to the electronic absorption studies, the crown-free analogues of **5** and **6** showed no changes in the emission characteristics upon the addition of Cs^+ ions, indicating that the crown pendants of the complexes are responsible for the association with Cs^+ ions. The stability constants were also obtained from the emission ion-binding data. The close resemblance of the experimental data to the theoretical fits further confirmed that the complexation of Cs^+ ion to the dinuclear Au(I) complex was in a 1:1 ratio. The log K_s value of 4.6 is in agreement with the value obtained from absorption measure-

(17) Bourson, J.; Pouget, J.; Valeur, B. *J. Phys. Chem.* **1993**, *97*, 4552.

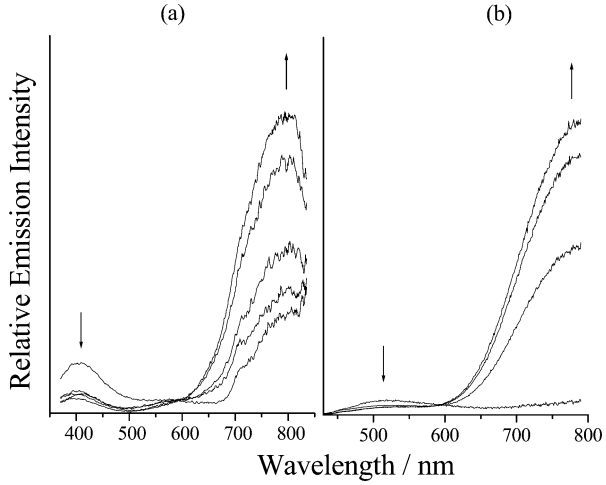

Figure 5. Corrected emission spectra of (a) $[Au_2(dppm)(S\text{-}B18C6)_2]$ (**4**) upon addition of various concentrations of CsOTf in CH_2Cl_2-MeOH (1:1, v/v) and (b) $[Au_2(dppm)(S\text{-}B15C5)_2]$ (**2**) upon addition of various concentrations of KPF_6 in CH_2Cl_2-MeOH (1:1, v/v).

ments. It is interesting to note that the lifetime of the excited state for the emission band at 790 nm was determined to be 0.14 μs, while the emission lifetime of the band at 410 nm in the absence of Cs^+ ions was found to be less than 0.1 μs. Although K^+ ions (ionic diameter: 2.66 Å) are well-known to have a high binding affinity to benzo-18-crown-6, addition of K^+ ions to $[Au_2(P\text{^}P)(S\text{-}B18C6)_2]$ did not give rise to the growth of a new emission band at 790 nm. Similarly, only a very small spectral change was observed in the UV−vis spectra, and no isosbestic points were obtained. The failure of the fit of the experimental data to a 1:1 complexation model suggested that the binding mode of K^+ ion may be in a 2:1 (2 K^+:Au_2) ratio, in which the K^+ ion would fit into the cavity of the benzo-18-crown-6 units.

In the case of $[Au_2(P\text{^}P)(S\text{-}B15C5)_2]$ (where P^P = dcpm, dppm) reported previously,[10] the unique luminescence response of these gold(I) thiolate complexes toward K^+ ion binding indicates the importance of metal−metal interactions in reporting the selective binding of metal ions into the bis-(crown) pocket. As shown in the corrected emission spectrum in Figure 5b, upon the successive addition of K^+ ions to **2**, a drop in emission intensity at ca. 502 nm with a concomitant formation of a new low-energy emission band at ca. 790 nm (uncorrected wavelength at 720 nm in ref 10) was observed, with an isoemissive point at ca. 600 nm. Figure 6 shows the excitation spectra of **2** in the absence and in the presence of potassium ions. The excitation spectra revealed that the high-energy emission band and the low-energy emission band came from different origins. The 502-nm emission band is originated from a higher energy absorption at 350 nm while the 790-nm emission band is derived from a lower energy absorption at ca. 400 nm. This observation is in agreement with the changes observed in the electronic absorption spectral traces upon addition of potassium ion. Addition of either Cs^+ or Rb^+ ions to **1** and **2** also gave similar emission spectral changes, with log K_s values of 3.4 and 2.3 obtained for **1** and **2**, respectively, upon addition of Cs^+ ions, while log K_s values of 3.4 and 2.9 were obtained, respectively, in the case of Rb^+ ions. These values are smaller

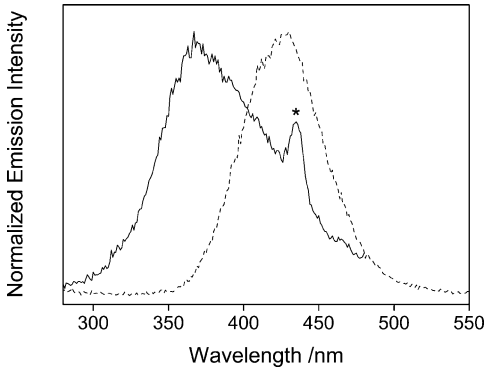

Figure 6. Excitation spectra of **2** in the absence (—) and in the presence (---) of potassium ions, monitored at 502 and 790 nm, respectively. (An asterisk denotes an instrumentation artifact.)

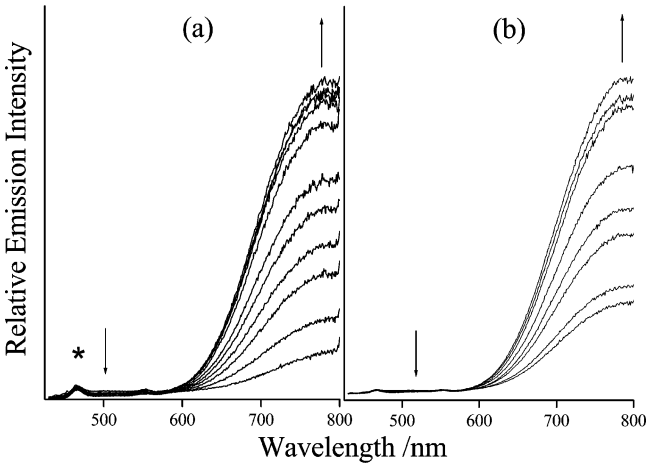

Figure 7. Corrected emission spectra of $[Au_2(dppm)(S\text{-}B15C5)_2]$ (**2**) upon addition of various concentrations of (a) CsOTf and (b) RbOTf in CH_2Cl_2-MeOH (1:1, v/v). (An asterisk denotes an instrumentation artifact.)

than the respective values obtained from K^+ ion-binding measurements. It is understandable that the cavity of benzo-15-crown-5 with diameter of 1.7−2.2 Å is most suitable to sandwich K^+ ion (ionic diameter: 2.66 Å) than either Cs^+ or Rb^+ ions which have larger ionic diameters of 3.34 and 2.98 Å, respectively. As a consequence, the log K_s values for $[Au_2(P\text{^}P)(S\text{-}B15C5)_2]$ with Cs^+ or Rb^+ ion-binding are found to be smaller than those with K^+ ions. The corrected emission spectral changes of **2** upon addition of various concentrations of CsOTf (a) and RbOTf (b) in CH_2Cl_2-MeOH (1:1, v/v) are depicted in Figure 7. The growth of a new low-energy emission band at ca. 790 nm upon addition of Cs^+ and Rb^+ ions was also observed. These observations were in line with the expectations when crown ethers with different cavity size were deliberately chosen in the design of such molecules, as variation in the crown size could alter the specificity toward various metal cations. In $[Au_2(P\text{^}P)(S\text{-}B18C6)_2]$, upon addition of Cs^+ or Rb^+ ions, which have ionic diameters too large to fit into the cavity of the benzo-18-crown-6, the Cs^+ or Rb^+ ions would tend to sandwich between the two crown moieties, similar to the sandwich binding mode that occurs in the case of benzo-15-crown-5 analogues with K^+ ions. As a result, the two Au(I) centers would be brought into close proximity, resulting in Au···Au interactions. As shown in Figure 8, the

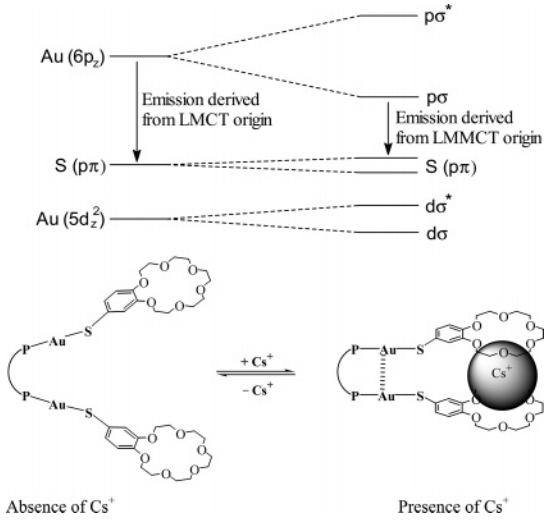

Figure 8. Schematic diagram of the orbital splittings and the proposed sandwich binding mode for cesium ion in $[Au_2(dcpm)(S\text{-}B18C6)_2]$ (**3**) and $[Au_2(dppm)(S\text{-}B18C6)_2]$ (**4**).

filled $5d_{z^2}$ and empty 6s and $6p_z$ orbitals on each Au atom would overlap with each other resulting from Au···Au interactions, which then gave rise to bonding and antibonding combinations of dσ, dσ*, sσ, sσ*, pσ, and pσ* character. A net stabilization of the dinuclear Au acceptor orbital of pσ parentage would result, leading to a new emission band in the red, characteristic of the thiolate-to-gold−gold ligand-to-metal−metal charge transfer (LMMCT) excited state. This is in accord with the observation of an excitation band at ca. 400 nm, attributed to a LMMCT absorption. On the contrary, in the absence of K^+ ions, complex **2** only shows an excitation band at ca. 350 nm, ascribed to a LMCT transition.

Although different metal cations (of different sizes) would be expected to give rise to a variation in the Au···Au distances in the sandwich adduct and hence emission energies, the observation that addition of K^+, Rb^+, and Cs^+ to **2** gave rise to an emission band of similar energy at ca. 790 nm is indicative of a similar Au···Au interaction irrespective of the size of the metal cation. This may be rationalized by the rather remote disposition of the benzocrown units from the Au(I) centers and the flexibility of the thiolate ligand which would become less effective in affecting the Au···Au distance, as well as the rigidity of the diphosphine bridging ligand as governed by the bite distance to afford a Au···Au separation that is rather preorganized and predetermined to give the best possible metal−metal interaction.

On the contrary, addition of an excess of free benzo[15]-crown-5 to the mixture of **2** and K^+ ions extracted the sandwiched K^+ ions from **2**, with a breaking of the short Au···Au contact and a reversal of the emission trend. Similarly, addition of Na^+ ions to a mixture of **2** and K^+ ions also caused a drop in the intensity of the emission band at 790 nm, probably as a result of the high affinity of the benzo[15]crown-5 unit for Na^+ ions, which displace the K^+ ions.

The variation of crown size on the gold(I) thiolate complexes is found to be useful for the specific recognition of metal ions, i.e. benzo-15-crown-5 for K^+, while benzo-18-crown-6 for Cs^+, through the on/off switching of Au···Au interactions, reported as luminescence signaling.

Table 5. Ion Clusters Observed in the Positive ESI-Mass Spectra of Various Complexes with Different Metal Cations

m/z	ion cluster
1415	$[Au_2(dppm)(S\text{-}B15C5)_2{\cdot}K]^+$
1597	$[Au_2(dppm)(S\text{-}B18C6)_2{\cdot}Cs]^+$
1641	$[\{Au_2(dppm)(S\text{-}B18C6)_2{\cdot}K_2\}(ClO_4)]^+$
771	$[Au_2(dppm)(S\text{-}B18C6)_2{\cdot}K_2]^{2+}$

Apart from spectrophotometric measurements, ESI-mass spectrometry provides another piece of evidence for the binding of metal cations to the complexes. The ESI-mass spectrometric results for the binding of various metal ions with different complexes were summarized in Table 5. Upon addition of various metal cations to the gold complexes, either 1:1 or 1:2 complexation adducts were observed, depending on the size of the metal ion and the preferred mode of binding. Only the 1:1 bound species, $[Au_2(dppm)(S\text{-}B18C6)_2{\cdot}Cs]^+$, was observed upon addition of excess cesium ion while mainly 1:2 adducts, $[Au_2(dppm)(S\text{-}B18C6)_2{\cdot}K_2]^{2+}$ and $[\{Au_2(dppm)(S\text{-}B18C6)_2{\cdot}K_2\}(ClO_4)]^+$, were found in the case of potassium ion addition. Similar findings have been observed in the mercaptobenzo-15-crown-5 analogues, in which the sandwich adduct, $[Au_2(dppm)(S\text{-}B15C5)_2{\cdot}K]^+$, was detected. These further support the complexation stoichiometry obtained from electronic absorption and emission studies.

Conclusion

As an extension of the work on novel dinuclear gold(I) phosphine complexes containing 4′-mercaptomonobenzo-15-crown-5 pendants, $[Au_2(P\text{^}P)(S\text{-}B15C5)_2]$ (P^P = dcpm, dppm), a series of gold(I) complexes with crown ethers of different cavity size have been synthesized so as to elucidate the perturbation of the ion-binding properties by different crown pendants.

All the dinuclear gold(I) complexes exhibited low-energy emissions in dichloromethane solution at room temperature, which have been assigned as originating from states derived from a S → Au ligand-to-metal charge transfer (LMCT) origin. The ion-binding properties of these complexes with various metal cations have been studied. Well-defined isosbestic points in the UV−vis absorption spectra were observed and the stability constants of the complexes with the metal cations have been determined. In the mercapto-crown ether-containing complexes, spectroscopic evidence has been provided for the metal ion-induced switching on of the gold···gold interactions upon metal ion binding. The corrected emission spectra of $[Au_2(dppm)(S\text{-}B18C6)_2]$ showed a drop in intensity at ca. 410 nm with the concomitant formation of a new low-energy emission band at ca. 790 nm upon addition of cesium ions. An isoemissive point was obtained at ca. 590 nm. The low-energy band was believed to originate from a thiolate-to-gold−gold ligand-to-metal−metal charge transfer (LMMCT) excited state as a result of the switching on of the Au···Au interaction upon cesium ion binding to the bis(benzo-18-crown-6) moiety which was

deliberately chosen in the design for the recognition of cesium ions, similar to the use of benzo-15-crown-5 in $[Au_2(P\hat{}P)(S\text{-}B15C5)_2]$ for the selective recognition of potassium ions. The binding of various metal cations to the complexes was further confirmed by ESI-mass spectrometry.

It is envisaged that with the rich spectroscopic and luminescence properties exhibited by d^{10} gold(I) complexes, together with the propensity of gold(I) centers to form weak Au···Au interactions resulting from aurophilicity, various gold(I) complexes capable of luminescence signaling could be designed by employing the appropriate bridging and ancillary ligands with special functions for the recognition of guest molecules. All this characteristic luminescence behavior would render the dinuclear gold(I) building block as an ideal candidate for the design of luminescence chemosensors as well as molecular optoelectronic switching devices on the basis of the switching on and off of the metal···metal interactions.

Experimental Section

Materials and Reagents. Benzo-15-crown-5,[18] 4′-mercaptobenzo-15-crown-5,[19] 4′-mercaptobenzo-18-crown-6,[19] $HAuCl_4 \cdot XH_2O$,[20] and $[Au_2(P\hat{}P)Cl_2]$ (P^P = dcpm, dppm)[21−23] were prepared according to reported procedures. 2,2′-Thiodiethanol, benzo-18-crown-6, bis(diphenylphosphino)methane, bis(dicyclohexylphosphino)methane, and tetra-*n*-butylammonium hexafluorophosphate were purchased from Aldrich Chemical Co., and the latter was recrystallized three times from hot ethanol prior to use. 3,4-Dimethoxybenzenethiol was obtained from Maybridge Chemical Co. Ltd. Dichloromethane (Lab Scan, AR) and diethyl ether (Lab Scan, AR) were purified and distilled using standard procedures before use.[24] All other reagents were of analytical grade and were used as received.

All reactions were carried out under strictly anhydrous and anaerobic conditions using standard Schlenk technique under an atmosphere of nitrogen.

Physical Measurements and Instrumentation. ^{1}H NMR spectra were recorded on a Bruker DPX-300 (300 MHz) FT-NMR spectrometer with chemical shifts reported relative to tetramethylsilane, $SiMe_4$. Positive ion fast-atom bombardment (FAB) mass spectra were recorded on a Finnigan MAT95 mass spectrometer. All electrospray-ionization (ESI) mass spectra were recorded on a Finnigan LCQ mass spectrometer. Elemental analyses of all newly synthesized metal complexes were performed on a Carlo Erba 1106 elemental analyzer at the Institute of Chemistry of the Chinese Academy of Sciences in Beijing. The electronic absorption spectra were recorded on a Hewlett-Packard 8452A diode-array spectrophotometer. Steady-state emission and excitation spectra recorded at room temperature and at 77 K were obtained on a Spex Fluorolog-2 model F111 fluorescence spectrophotometer with or without Corning filters and were corrected for instrumental responses. All solutions for photophysical studies ($\sim 10^{-5}$ mol dm^{-3}) were prepared under high vacuum in a 10-cm^3 round-bottomed flask equipped with a sidearm 1-cm fluorescence cuvette and sealed from the atmosphere by a Rotaflo HP6/6 quick-release Teflon stopper. Solutions were rigorously degassed on a high-vacuum line in a two-compartment cell with no less than four successive freeze−pump−thaw cycles. Solid-state photophysical measurements were carried out with the solid sample loaded in a quartz tube inside a quartz-walled Dewar flask. Liquid nitrogen was placed into the Dewar flask for low-temperature (77 K) solid-state and glass photophysical measurements. Emission-lifetime measurements were performed using a conventional laser system. The excitation source was the 355 nm output (third harmonic) of a Spectra-Physics Quanta-Ray Q-switched GCR-150-10 pulsed Nd:YAG laser. Luminescence decay signals from a Hamamatsu R928 photomultiplier tube were converted to voltage changes by connecting to a 50Ω load resistor and were then recorded on a Tektronix model TDS-620A digital oscilloscope. The lifetime τ was determined by a single-exponential fitting of the luminescence decay trace with the relationship $I = I_o \exp(-t/\tau)$, where I and I_o are the luminescence intensity at time = t and 0, respectively. Solution samples for luminescence lifetime measurements were degassed by no less than four successive freeze−pump−thaw cycles.

Binding Constant Determination. The concentrations of the gold complexes employed in the UV−vis and emission titration studies are typically in the range of 4×10^{-5} to 1×10^{-4} mol dm^{-3}. The electronic absorption spectral titration for binding constant determination was performed on a Hewlett-Packard 8425A diode-array spectrophotometer at 25 °C which was controlled by a Lauda RM6 compact low-temperature thermostat. Supporting electrolyte (0.1 mol dm^{-3} ^{n}Bu$_4$NPF$_6$) was added to maintain the ionic strength of the sample solution constant during the titration to avoid any changes in the ionic strength of the medium.

Binding constants for 1:1 complexation were obtained according to[17]

$$X = X_o + \frac{X_{lim} - X_o}{2[C_o]}([C_o] + [C_m] + 1/K_s - \{([C_o] + [C_m] + 1/K_s)^2 - 4[C_o][C_m]\}^{1/2}) \quad (1)$$

where X_o and X are the absorbance of the complex at a selected wavelength in the absence and presence of the metal cation, respectively, $[C_o]$ is the total concentration of the complex, $[C_m]$ is the concentration of the metal cation, X_{lim} is the limiting value of absorbance in the presence of excess metal ion, and K_s is the stability constant.

From the emission binding data, binding constants were also obtained using eq 3 by the modification of eq 2 as follows:[17]

$$I = I_o + \frac{I_{lim} - I_o}{2[C_o]}([C_o] + [C_m] + 1/K_s - \{([C_o] + [C_m] + 1/K_s)^2 - 4[C_o][C_m]\}^{1/2}) \quad (2)$$

Here I_o and I are the emission intensity of the complex at a selected wavelength λ in the absence and presence of the metal cation, respectively, $[C_o]$ is the total concentration of the complex, $[C_m]$ is the concentration of the metal cation, I_{lim} is the limiting value of absorbance in the presence of excess metal ion, and K_s is the stability constant.

Syntheses of Mercaptocrown Ether-Containing Complexes. $[Au_2(dcpm)(S\text{-}B15C5)_2]$ (1). To a solution of $[Au_2(dcpm)Cl_2]$ (30

(18) Pedersen, C. J. *J. Am. Chem. Soc.* **1967**, *89*, 7017.
(19) (a) Shinkai, S.; Minami, T.; Araragi, Y.; Manabe, O. *J. Chem. Soc., Perkin Trans.* **1985**, 503. (b) Nabeshima, T.; Hanami, T.; Akine, S.; Saiki, T. *Chem. Lett.* **2001**, 560.
(20) Block, B. P.; Bartkiewicz, S. A.; Chrisp, J. D. *Inorg. Synth.* **1953**, *4*, 14.
(21) Yam, V. W. W.; Chan, C. L.; Cheung, K. K. *J. Chem. Soc., Dalton Trans.* **1996**, 4019.
(22) Yam, V. W. W.; Choi, S. W. K. *J. Chem. Soc., Dalton Trans.* **1994**, 2057.
(23) Schmidbaur, H.; Wohlleben, A.; Wagner, F.; Orama, O.; Huttner, G. *Chem. Ber.* **1977**, *110*, 1748.
(24) Perrin, D. D.; Armarego, W. L. F. *Purification of Laboratory Chemicals*, 3rd ed.; Pergamon: Oxford, U.K.

mg, 0.034 mmol) in dichloromethane (5 mL) was added a mixture of 4′-mercaptomonobenzo-15-crown-5 (21 mg, 0.071 mmol) and triethylamine (40 μL, 0.29 mmol). The reaction mixture was stirred for 30 min at room temperature, after which the solvent was removed under reduced pressure. The pale yellow residue was dissolved in dichloromethane. Recrystallization of the complex by the diffusion of diethyl ether vapor into a dichloromethane solution yielded **1** as pale yellow crystals (32 mg, 0.022 mmol, 67% yield). ^{1}H NMR (300 MHz, $CDCl_3$, 298 K): δ 1.10−2.23 (m, 44H, $-C_6H_{11}$; 2H, $-PCH_2P-$), 3.74 (m, 16H, $-OCH_2-$), 3.90 (m, 8H, $-C_6H_3OCH_2CH_2-$), 4.10 (m, 8H, $-C_6H_3OCH_2-$), 6.62 (d, 2H, J = 8.3 Hz, aryl H *meta* to S), 7.05−7.10 (m, 4H, aryl H *ortho* to S). Positive-ion FAB mass spectrum: *m*/*z* 1101, $[M - (S\text{-}B15C5)]^+$. Anal. Found: C, 44.28; H, 5.88. Calcd for $C_{53}H_{84}Au_2O_{10}P_2S_2 \cdot 1/2CH_2Cl_2$: C, 44.53; H, 5.89.

[Au$_2$(dppm)(S-B15C5)$_2$] (2). The procedure was similar to that described for the preparation of **1** except [Au$_2$(dppm)Cl$_2$] (29 mg, 0.034 mmol) was used in place of [Au$_2$(dcpm)Cl$_2$]. Recrystallization of the complex by the diffusion of diethyl ether vapor into a dichloromethane solution yielded **2** as yellow solid (35 mg, 0.025 mmol, 74% yield). ^{1}H NMR (300 MHz, $CDCl_3$, 298 K): δ 3.70 (m, 16H, $-OCH_2-$; 2H, $-PCH_2P-$), 3.90 (m, 8H, $-C_6H_3OCH_2CH_2-$), 4.10 (m, 8H, $-C_6H_3OCH_2-$), 6.62 (d, 2H, J = 8.3 Hz, aryl H *meta* to S), 7.05−7.10 (m, 4H, aryl H *ortho* to S), 7.24−7.70 (m, 20H, $-PPh_2$). Positive-ion FAB mass spectrum: *m*/*z* 1077, $[M - (S\text{-}B15C5)]^+$. Anal. Found: C, 42.89; H. 3.91. Calcd for $C_{53}H_{60}Au_2O_{10}P_2S_2 \cdot 2CH_2Cl_2$: C, 42.71; H, 4.14.

[Au$_2$(dcpm)(S-B18C6)$_2$] (3). The procedure was similar to that described for the preparation of **1** except 4′-mercaptomonobenzo-18-crown-6 (25 mg, 0.073 mmol) was used in place of 4′-mercaptomonobenzo-15-crown-5. Recrystallization of the complex by the diffusion of diethyl ether vapor into a dichloromethane solution yielded **3** as pale yellow crystals (32 mg, 0.022 mmol, 65% yield). ^{1}H NMR (300 MHz, $CDCl_3$, 298 K): δ 1.10−2.25 (m, 44H, $-C_6H_{11}$; 2H, $-PCH_2P-$), 3.70 (m, 24H, $-OCH_2-$), 3.85 (m, 8H, $-C_6H_3OCH_2CH_2-$), 4.10 (m, 8H, $-C_6H_3OCH_2-$), 6.61 (d, 2H, J = 8.3 Hz, aryl H *meta* to S), 7.05−7.15 (m, 4H, aryl H *ortho* to S). Positive-ion FAB mass spectrum: *m*/*z* 1488, $[M + H]^+$. Anal. Found: C, 45.35; H, 6.15. Calcd for $C_{57}H_{92}Au_2O_{12}P_2S_2 \cdot 1/2CH_2Cl_2$: C, 45.09; H, 6.12.

[Au$_2$(dppm)(S-B18C6)$_2$] (4). The procedure was similar to that described for the preparation of **2** except 4′-mercaptomonobenzo-18-crown-6 (25 mg, 0.073 mmol) was used in place of 4′-mercaptomonobenzo-15-crown-5. Recrystallization of the complex by the diffusion of diethyl ether vapor into an acetone solution yielded **4** as pale yellow solid (32 mg, 0.022 mmol, 65% yield). ^{1}H NMR (300 MHz, $CDCl_3$, 298 K): δ 3.70 (m, 24H, $-OCH_2-$; 2H, $-PCH_2P-$), 3.85 (m, 8H, $-C_6H_3OCH_2CH_2-$), 4.10 (m, 8H, $-C_6H_3OCH_2-$), 6.65 (d, 2H, J = 8.3 Hz, aryl H *meta* to S), 7.05−7.15 (m, 4H, aryl H *ortho* to S), 7.25−7.65 (m, 20H, $-PPh_2$). Positive-ion FAB mass spectrum: *m*/*z* 1122, $[M - (S\text{-}B18C6)]^+$. Anal. Found: C, 47.14; H, 4.75. Calcd for $C_{57}H_{92}Au_2O_{12}P_2S_2 \cdot (CH_3)_2CO$: C, 47.31; H, 4.90.

[Au$_2$(dcpm)(SC$_6$H$_3$(OMe)$_2$-3,4)$_2$] (5). The procedure was similar to that described for the preparation of **1** except 3,4-dimethoxybenzenethiol (12 mg, 0.071 mmol) was used in place of 4′-mercaptomonobenzo-15-crown-5. Recrystallization of the complex by the diffusion of diethyl ether vapor into dichloromethane solution yielded **5** as yellow solid (23 mg, 0.021 mmol, 61% yield). ^{1}H NMR (300 MHz, $CDCl_3$, 298 K): δ 1.10−2.20 (m, 44H, $-C_6H_{11}$; 2H, $-PCH_2P-$), 3.79 (s, 6H, $-OCH_3$), 3.84 (s, 6H, $-OCH_3$), 6.60 (d, 2H, J = 8.2 Hz, aryl H *meta* to S), 7.02−7.10 (m, 4H, aryl H *ortho* to S). Positive-ion FAB mass spectrum: *m*/*z* 971, $[M - (SC_6H_3(OMe)_2)]^+$. Anal. Found: C, 40.21; H, 5.21. Calcd for $C_{41}H_{64}Au_2O_4P_2S_2 \cdot CH_2Cl_2 \cdot H_2O$: C, 40.57; H, 5.47.

[Au$_2$(dppm)(SC$_6$H$_3$(OMe)$_2$-3,4)$_2$] (6). The procedure was similar to that described for the preparation of **2** except 3,4-dimethoxybenzenethiol (12 mg, 0.071 mmol) was used in place of 4′-mercaptomonobenzo-15-crown-5. Recrystallization of the complex by the diffusion of diethyl ether vapor into dichloromethane solution yielded **6** as yellow solid (24 mg, 0.021 mmol, 65% yield). ^{1}H NMR (300 MHz, $CDCl_3$, 298 K): δ 3.70 (s, 2H, $-PCH_2P-$), 3.80 (s, 12H, $-OCH_3$), 6.60 (d, 2H, J = 8.0 Hz, aryl H *meta* to S), 7.05−7.10 (m, 4H, aryl H *ortho* to S), 7.20−7.40, 7.60−7.70 (m, 20H, $-PPh_2$). Positive-ion FAB mass spectrum: *m*/*z* 947, $[M - (SC_6H_3(OMe)_2)]^+$. Anal. Found: C, 43.94; H, 3.67. Calcd for $C_{41}H_{40}Au_2O_4P_2S_2$: C, 44.11; H, 3.58.

Crystal Structure Determination. Single crystals of [Au$_2$(dcpm)(S-B15C5)$_2$] (**1**) and [Au$_2$(dcpm)(S-B18C6)$_2$] (**3**) were obtained from the slow diffusion of diethyl ether vapor into the dichloromethane solution of the corresponding compounds. For **1**, X-ray diffraction data were collected at 28 °C on a Rigaku AFC7R diffractometer with graphite-monochromatized Mo Kα radiation (λ = 0.710 73 Å) using $\omega-2\theta$ scans with ω-scan angle (0.73 + 0.35 tan θ)° at a scan speed of 8.0 deg min^{-1} (up to 6 scans for reflections with $I < 15\sigma(I)$). Intensity data (in the range of $2\theta_{max}$ = 50°; *h*, 0 to 19; *k*, 0 to 23; *l*, −20 to 20; 3 standard reflections measured after every 300 reflections showed decay of 0.71%) were corrected for Lorentz and polarization effects. A total of 10 977 reflections were measured, of which 10 587 were unique and R_{int} = 0.045. A total of 4415 reflections with $I > 3\sigma(I)$ were considered observed and used in the structural analysis. The space group was uniquely determined on the basis of systematic absences, and the structure was solved by Patterson methods and expanded by Fourier methods (PATTY[25]) and refinement by full-matrix least-squares using the software package TeXsan.[26] Convergence for 307 variable parameters by least-squares refinement on F with $w = 4F_o^2/\sigma^2(F_o^2)$, where $\sigma^2(F_o^2) = [\sigma^2(I) + (0.026F_o^2)^2]$ for 4415 reflections with $I > 3\sigma(I)$, was reached at R = 0.047 and wR = 0.069 with a goodness-of-fit of 2.60. $(\Delta/\sigma)_{max}$ = 0.05 except for atoms of the two crown ether parts having large temperature factors. For **3**, X-ray diffraction data were collected at 20 °C on a MAR diffractometer with a 300 mm image plate detector using graphite-monochromatized Mo Kα radiation (λ = 0.710 73 Å). Data collection was made with 2° oscillation step of φ, 600 s exposure time, and scanner distance at 120 mm. A total of 90 images were collected. The images were interpreted and intensities integrated using program DENZO.[27] The structure was solved by direct methods employing the SIR-97[28] program. Gold, sulfur, phosphorus, and many non-hydrogen atoms were located according to the direct methods and the successive least-squares Fourier cycles. According to the SHELXL-97[29] program, all 9324 independent reflections (R_{int} equal to 0.0601, 4821 reflections larger than $4\sigma(F_o)$, where $R_{int} = \Sigma|F_o^2 - F_o^2(\text{mean})|/\Sigma[F_o^2]$) from a total 27 329 reflections were partici-

(25) Beurskens, P. T.; Admiraal, G.; Beurskens, G.; Nosman, W. P.; Garcia-Granda, S.; Gould, R. O.; Smits, J. M. M.; Smykalla, C. *The DIRDIF Program System*; Technical Report of the Crystallography Laboratory; University of Nijmegen: Nijmegen, The Netherlands, 1992.
(26) *Crystal Structure Analysis Package*; Molecular Structure Corp.: The Woodlands, TX, 1985 and 1992.
(27) Otwinowski, Z.; Minor, W. *Methods Enzymol.* **1997**, *276*, 307.
(28) Sir97: a new tool for crystal structure determination and refinement. Altomare, A.; Burla, M. C.; Camalli, M.; Cascarano, G.; Giacovazzo, C.; Guagliardi, A.; Moliterni, A. G. G.; Polidori, G.; Spagna, R. *J. Appl. Crystallogr.* **1998**, *32*, 115.
(29) SHELXL97: Sheldrick, G. M. *SHELXL97: Programs for Crystal Structure Analysis*, release 97-2; University of Göttingen: Goöttingen, Germany, 1997.

pated in the full-matrix least-squares refinement against F^2. These reflections were in the range $-21 \leq h \leq 21$, $-23 \leq k \leq 23$, and $-18 \leq l \leq 17$ with $2\theta_{max}$ equal to 50.68°. Convergence $((\Delta/\sigma)_{max} = -0.001$, average 0.001) for 545 variable parameters by full-matrix least-squares refinement on F^2 reaches $R_1 = 0.0475$ and $wR_2 = 0.1223$ with a goodness-of-fit of 0.877.

Acknowledgment. V.W.-W.Y. acknowledges support from the University Grants Committee of Hong Kong Special Administration Region, China (Project AoE/P-10/01); the University Development Fund of The University of Hong Kong; and The University of Hong Kong Foundation for Education Development and Research Limited, and C.-K.L. acknowledges the receipt of a Postgraduate Studentship, administered by The University of Hong Kong. The work has been supported by a CERG Grant from the Research Grants Council of the Hong Kong Special Administrative Region of China (Project No. HKU 7020/02P).

Supporting Information Available: Tables giving atomic coordinates, anisotropic thermal parameters, bond lengths, and bond angles for complexes **1** and **3** (CIF) and a positive ESI mass spectrum of a CH_2Cl_2-MeOH (1:1, v/v) solution of **4** and excess CsOTf. This material is available free of charge via the Internet at http://pubs.acs.org.

IC049094U